Defense Technical Information Center
Compilation Part Notice

ADP013679

TITLE: Direct Numerical Simulation of Jet Noise

DISTRIBUTION: Approved for public release, distribution unlimited

This paper is part of the following report:

TITLE: DNS/LES Progress and Challenges. Proceedings of the Third
AFOSR International Conference on DNS/LES

To order the complete compilation report, use: ADA412801

The component part is provided here to allow users access to individually authored sections
of proceedings, annals, symposia, etc. However, the component should be considered within
the context of the overall compilation report and not as a stand-alone technical report.

The following component part numbers comprise the compilation report:
ADP013620 thru ADP013707

DIRECT NUMERICAL SIMULATION OF JET NOISE

BENDIKS JAN BOERSMA

J.M. Burgers Centre
Delft University of Technology
Mekelweg 2
2628 CD Delft
The Netherlands
email: b.j.boersma@wbmt.tudelft.nl

Abstract. In this paper we will investigate the sound field of a round turbulent jet with a Mach number of 0.6 based on the jet centerline velocity and the ambient speed of sound. The sound field is obtained by solving a wave equation for the acoustic field. Two different acoustic source terms are used as right hand side of the wave equation. One in which the source term is given by traditional Lighthill stress tensor and a second one in which the source term is based on the vorticity in the fluid.

1. Introduction

A generic flow geometry of aeroacoustical sound production is a turbulent jet. Most people will be familiar with the sound of a jet engine of a commercial airliner. Stricter environmental measures around airports have put strong limitations on the sound that may produced by jets. Although significant sound reduction of these jet engines has been obtained over the last few decades, it is nevertheless required to reduce the sound of jet engines even more in view of the strong growth in air traffic foreseen in the future. The above mentioned jet engine is only one of the examples and other examples are aeroacoustical sound produced by high speed trains, wind noise around buildings, the sound comfort in cars but also ventilator noise in various household appliances. In this study we will focus on sound produced by turbulent jets because this flow is one of the benchmark flows for which a reasonable amount of experimental data is available.

Here we only want to mention the experimental studies which are relevant for this study, for a more detailed overview we refer to Goldstein (1976). Lush (1971) reports acoustic pressure spectra of a Mach 0.3, 0.6 and 0.9 turbulent jet. Mollo-Christensen (1967) also reports spectra for Mach 0.6 and Mach 0.9 turbulent jets and gives detailed information about the directivity of the sound. Unfortunately no information is given on the structure of the flow field. Information on the flowfield of a jet has been presented in various studies see for instance, Panchapekesan & Lumley (1993), and Boersma *et al.* (1998). There is as far as we know, no detailed experimental study in which both the flow field and the acoustic field are presented.

Recently, with increasing computer power, it has become possible to calculate the acoustic field of simple flows using Direct Numerical Simulation (DNS), Colonius *et al.* (1997), Mitchell *et al.* (1999). Direct numerical simulations of high Mach number turbulent jets have been performed by Freund (1998). In these simulations the sound is calculated with help of Kirchhoff surfaces. In low Mach number flows the acoustic amplitudes are very small and it is likely that acoustic equations like the one proposed by Lighthill (1952) or Howe (1975) will give more reliable results which are less contaminated by numerical errors.

In this paper we will focus on a jet with a Mach number of 0.6. We will compare acoustic fields obtained with both the Lighthill and Howe equations.

2. Governing equations

The flow is described by the well known compressible Navier-Stokes equations which can be found in various text books (Bachelor 1967). The equation for conservation of mass reads.

$$\frac{\partial \rho}{\partial t} + \frac{\partial \rho u_i}{\partial x_i} = 0 \tag{1}$$

where ρ is the fluids density and u_i the fluids velocity component in the ith coordinate direction. The equation which describes the conservation of momentum reads

$$\frac{\partial \rho u_i}{\partial t} + \frac{\partial \rho u_j u_i}{\partial x_j} = -\frac{\partial p}{\partial x_i} + \frac{\partial}{\partial x_i} \tau_{ij} \tag{2}$$

In which p is the pressure and τ_{ij} is the viscous stress given by:

$$\tau_{ij} = \mu S_{ij} = \mu \left(\frac{\partial u_i}{\partial x_j} + \frac{\partial u_j}{\partial x_i} - \frac{2}{3}\delta_{ij}\frac{\partial u_i}{\partial x_i} \right) \tag{3}$$

The dynamics viscosity μ is a weak function of the temperature in the gas. For the moment we will neglect this and assume that μ is constant.

For the energy equation in a compressible flow various formulations are possible. Here we choose for a formulation using the total energy, i.e. the sum of temperature and kinetic energy

$$E = \rho C_v T + \frac{1}{2}\rho u_i u_i \tag{4}$$

In which C_v is the specific heat at constant volume and T the temperature. The transport equation for the total energy E reads

$$\frac{\partial E}{\partial t} + \frac{\partial}{\partial x_i} u_i [E + p] = \frac{\partial}{\partial x_i} \kappa \left(\frac{\partial T}{\partial x_i} \right) + \frac{\partial}{\partial x_i} u_i S_{ij} \tag{5}$$

In which κ is the thermal diffusion coefficient, which is again a weak function of the fluids temperature. The formulation of the energy equation given above has the advantage that no source terms appear in the right hand side which would be the case for formulations using the temperature instead of the energy. The temperature T, the pressure p and the density ρ are related to each other by the equation of state

$$p = \rho R T \tag{6}$$

2.1. THE ACOUSTIC FIELD

The acoustic field of the jet can be calculated with help of acoustic analogons like the Lighthill equation (Goldstein 1976):

$$\frac{\partial^2 \rho'}{\partial t^2} + c^2 \frac{\partial^2 \rho'}{\partial x_i^2} = \frac{\partial^2}{\partial x_i \partial x_j} T_{ij}. \tag{7}$$

In which ρ' is the acoustic density of the gas, c the speed of sound and T_{ij} is the Lighthill stress tensor which is given by the following relation

$$T_{ij} = \rho u_i u_j + \mu \left(\frac{\partial u_i}{\partial x_j} + \frac{\partial u_j}{\partial x_i} \right). \tag{8}$$

For turbulent flows the viscous term in the Lighthill stress tensor will be small and T_{ij} can be approximated by $T_{ij} \approx \rho u_i u_j$. Furthermore, if the Mach number is sufficiently small the density ρ can be replaced by the ambient value ρ_∞, resulting in the following equation for the acoustic density fluctuations

$$\frac{\partial^2 \rho}{\partial t^2} + c^2 \frac{\partial^2 \rho}{\partial x_i^2} = \rho_\infty \frac{\partial^2}{\partial x_i \partial x_j} u_i u_j. \tag{9}$$

Another formulation of the wave equation has been proposed by (Howe 1975). In this formulation the Lighthill tensor is expressed in terms of the vorticity and kinetic energy.

$$\frac{\partial^2}{\partial x_i \partial x_j} u_i u_j = \nabla \cdot \nabla \cdot (\underline{u}\,\underline{u}) = \nabla \cdot (\underline{\omega} \times \underline{u}) + \nabla^2 \frac{1}{2} u^2 \qquad (10)$$

For low Mach number flows the last term in the equation above (the kinetic energy) is neglected (Howe 1975) and we find the following wave equation for the sound

$$\frac{\partial^2 \rho}{\partial t^2} + c^2 \frac{\partial^2 \rho}{\partial x_i^2} = \nabla \cdot (\underline{\omega} \times \underline{u}) \qquad (11)$$

3. Numerical method

In the previous section we have presented the governing equation for compressible flow. In this section we will describe how those equations are discretized.

A natural choice for the computation of a round jet would be to use a cylindrical coordinate system. In previous computational studies such systems have been used, Freund (1998), Boersma et al. (1998). The problem when dealing with such a coordinate system is the treatment of the singularity at the centerline ($r = 0$) of the coordinate system. In the literature various methods are discussed, for a detailed overview we refer to Mohensi & Colonius (2000). None of these methods are able to retain a high order of numerical accuracy at the axis ($r = 0$) of the system. In physical space this axis will represent the jet centerline. An accurate simulation at the jet centerline is necessary because this is the area where most of the sound will be produced. In view of the problems mentioned above we have decided to use a Cartesian coordinate system for the complete flow domain.

The computational grid in the physical domain is non-uniform. Mapping functions $X_i = \eta_i(x_i)$, with $X_i = i\Delta X$ are used to map differential equation on a uniform grid in the computational domain, i.e.

$$\frac{\partial f}{\partial x} = \frac{\partial f}{\partial X} \frac{\partial X}{\partial x} \qquad (12)$$

The mapping function $X_i = \eta_i(x_i)$ is chosen in such a way that $\partial X/\partial x$ can be integrated analytically to obtain the physical distribution of the gridpoints x_i. The derivative $\partial f/\partial X$ has been calculated with a 8th order compact finite difference scheme (Lele 1992):

$$\left.\frac{\partial f}{\partial X}\right|_i = f_i' \qquad (13)$$

$$\frac{3}{8}\left(f_{i-1}' + f_{i+1}'\right) + f_i' = \frac{25}{32}\frac{f_{i+1} - f_{i-1}}{\Delta X} + \frac{3}{60}\frac{f_{i+2} - f_{i-2}}{\Delta X} - \frac{1}{480}\frac{f_{i+3} - f_{i-3}}{\Delta X}$$

At the boundaries of the computational domain the accuracy of the compact scheme was reduced to third order, (Lele 1992). If we would have used a cylindrical system we would also have to reduce the order at the jet centerline to third order. Which on its turn would give an unreliable prediction of T_{ij}.

All the spatial derivatives in the continuity, momentum and energy equation are discretized with the 8th order approximation given above. The time integration has been performed with a standard 4th order Runga-Kutta method. The time step was fixed and the corresponding CFL number $(u_i \Delta t / \Delta x_i)$ was approximately 1.0

Two different computational domains are used, one with a small spatial size for the Navier-Stokes equations and one with a larger spatial size for the wave equations. The Navier-Stokes domain consisted of $160 \times 144 \times 144$ the x, y and z-direction respectively (x is streamwize direction). The wave domain consisted of $320 \times 272 \times 272$ points.

4. Results

In this section we will present results obtained from the Direct Numerical Simulation of the jet and the sound field. For the jet-inflow profile a simple hyperbolic tangent profile of the following form is taken

$$U(r) = Ma \left(\frac{1}{2} - \frac{1}{2} \tanh[20(r - R_0)] \right) \tag{14}$$

In which R_0 is the radius of the jet and Ma the Mach number. The calculations have been continued until they reached a statistically steady state. After the calculations have reached this state they are continued for another 200 acoustic timescales R_0/c to obtain the statistics.

In Figure 1 (left) we show an instantaneous plot of the density field ρ in the jet and in Figure 1 (right) a contour plot of the total energy E in the jet. The figures show that the flow is laminar close to the jet nozzle and starts to become turbulent in the region $10 < x/R_0 < 15$ and becomes gradually fully turbulent farther downstream of the jet nozzle. In Figure 2 we show the mean velocity profiles along the jet centerline. In the region close to the jet orifice the centerline velocity is constant and then suddenly drops. The point were the centerline velocity suddenly drops is the point were most of the sound will be produced.

In Figure 3 (left) an instantaneous plot of the right hand side of equation (9) is shown. In Figure 3 (right) the right hand side of equation (11) has been plotted. Clearly there is a large difference between both source terms close to the jet nozzle. The source terms are large in the region $10 < x/R_0 < 30$, i.e the region in which the flow goes from a laminar to a turbulent state.
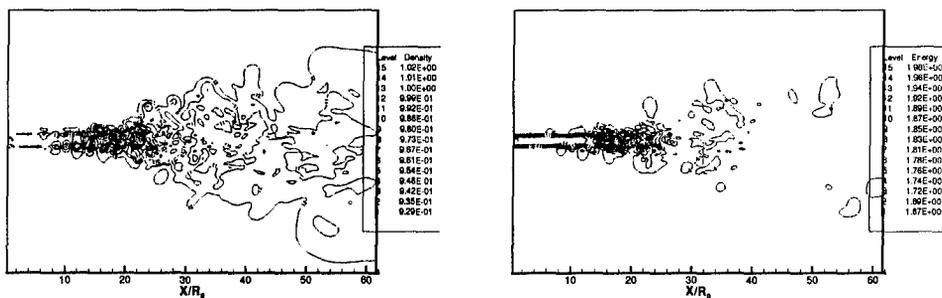
Figure 1. Left: an instantaneous plot of the density in the jet, right: an instantaneous plot of the axial velocity.
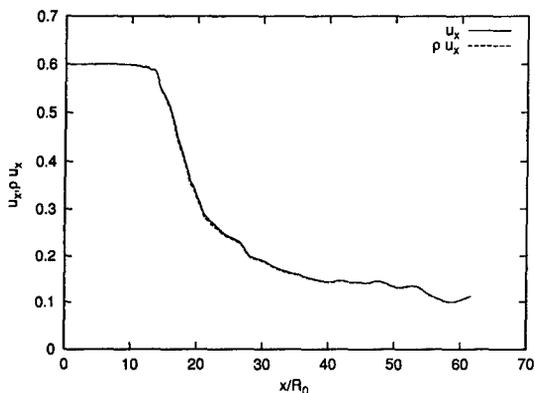
Figure 2. The mean axial velocity and axial flux at the jet centerline as a function of the downstream coordinate.

The difference between the two source terms is due to the removal of the kinetic energy from the right hand side of equation (10) and therefore the difference between the source terms are most pronounced in regions with a relatively large velocity, i.e. the region close to the centerline of the jet.

In Figure 4 the acoustic fields obtained with equations (9) and (11) are shown (the acoustic field is visualized with help of the dillatation $q = \partial \rho'/\partial t$). The sound field obtained with help of the Lighthill equations is very similar to the sound field observed in experiments. For instance, most of the sound is emitted under an angle of approximately 30° which is also found in the experiments by Lush (1971) and Mollo-Christensen (1967). The second result presented in Figure 4 clearly has a wrong directivaty pattern and too much sound is emitted under and angle of 90°.
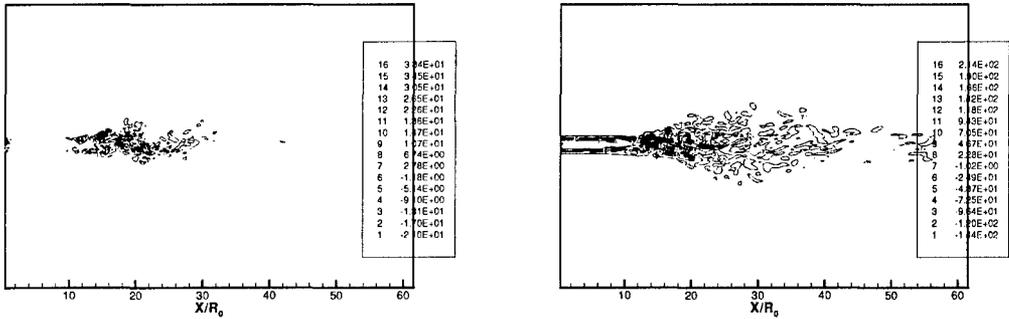
Figure 3. The acoustic source terms. Left: the right hand side of equation (9), Right: the right hand side of equation (11).

5. Conclusion

In this paper we have presented the sound field produced by a turbulent jet using two different acoustic equations. One of these equation is the traditional Lighthill equation which relates the sound to Reynolds stresses in the fluid. The second formulation we have used has been derived by Howe and relates the sound in the fluid to the vorticity. The last formulation is often preferred because it can be used in combination with simple vortex models for the flow, see e.g. Howe (1975).

It has been shown that there is a considerable difference between the source terms in the two formulations. The directivity pattern of the acoustic field obtained with equation (9) is much better than the pattern obtained with equation (11).

References

Batchelor, G.K., 1967, *An introduction to fluid mechanics*, Cambridge University Press.

Boersma, B.J., Brethouwer, G., and Nieuwstadt, F.T.M, 1998, A numerical investigation on the effect of the inflow conditions on the the self-similar region of a round jet, *Physics of Fluids* 10, 899-909.

Colonius, T., Lele, S.K., & Moin, P., 1997, Sound generation in a mixing layer, *J. Fluid Mech*, **330**, 375-409.

Freund, J.B., Lele, S.K., & Moin, P., 1998, Direct simulation of a Mach 1.92 jet and its sound field, AIAA/CEAS paper 98-2291.

Goldstein, M.E., 1976, *Aeroacoustics* McGraw Hill.

Howe, M.S., 1975, Contributions to the theory of aerodynamics sound, with application to excess jet noise and the theory of the flute, *J. Fluid Mech.*,**71**, 625-673.

Lele, S.K., 1992, Compact finite difference schemes with spectral-like resolution, *J. Comp. Phys.* 103, 16-42.

Lighthill, M.J., 1952, On sound generated aerodynamically, *Proc. R. Soc. of London Ser. A*, 211, 564-587.
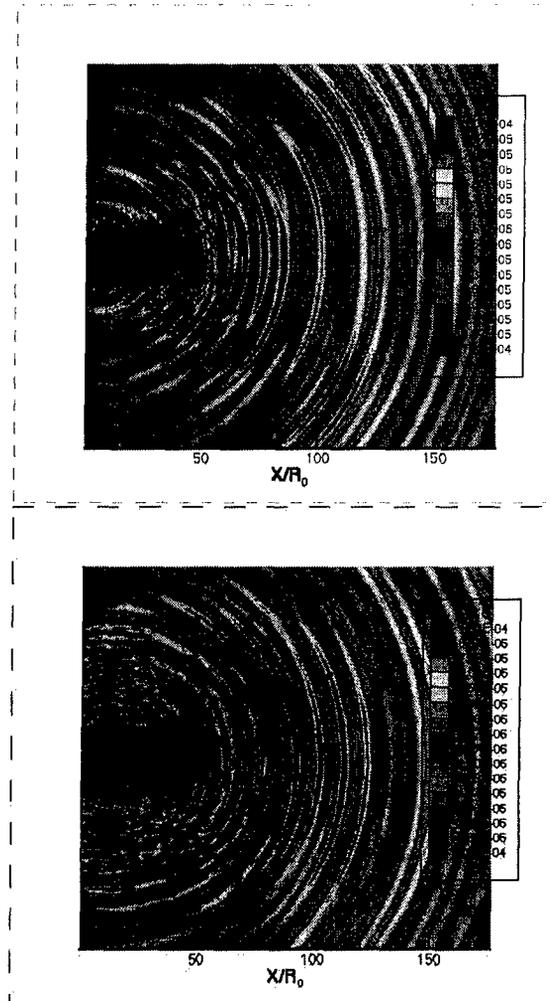
Figure 4. The acoustic field obtained with equation 9 (top) and with help of equation 11 (bottom).

Lighthill, M.J., 1954, On sound generated aerodynamically: II. Turbulence as a source of sound.*Proc. R. Soc. of London, Ser. A,* 222, 1-32.

Lush., P.A., 1971, Measurement of subsonic jet noise and comparison with theory, *J. Fluid Mech.*, **46**, 477-500.

Mitchell, B.E., Lele, S.K., Moin, P., 1999, Direct computation of the sound generated by vortex pairing in an axissymmetric jet, *J. Fluid Mech,* **383**, 113-142.

Mohensi, K. & Colonius, T., 2000, Numerical Treatment of Polar coordinate singularities, *J. Comp. Phys.*, **157**, 787-795.

Mollo-Christensen, E., 1967, Jet noise and shear flow instabilities seen from an experimenter's viewpoint, *J. Appl. Mech.*, **34**, 1-7.

Panchapakesan, N.R., and Lumley, J.L., 1993 *Turbulence measurements in axissymmetric jets of air and helium. Part 1. Air jet,* J. Fluid Mech. i**246**, 197-224.